Comparative Analysis of Urban Atmospheric Aerosol by Particle-Induced X-ray Emission (PIXE), Proton Elastic Scattering Analysis (PESA), and Aerosol Mass Spectrometry (AMS)

K. S. JOHNSON,[*,†,#] A. LASKIN,[‡] J. L. JIMENEZ,[§] V. SHUTTHANANDAN,[‡] L. T. MOLINA,[†,∥] D. SALCEDO,[⊥] K. DZEPINA,[§] AND M. J. MOLINA[†,▽]

Department of Chemistry, Massachusetts Institute of Technology, Cambridge, Massachusetts 02139, William R. Wiley Environmental Molecular Sciences Laboratory, Pacific Northwest National Laboratory, P.O. Box 999, MSIN K8-88, Richland, Washington 99352, Department of Chemistry and Biochemistry and CIRES, University of Colorado, Boulder, Colorado 80309, Molina Center for Energy and the Environment, La Jolla, California 92037, and Centro de Investigaciones Químicas, Universidad Autonoma del Estado de Morelos, Cuernvaca, Mexico 62210

Received February 7, 2008. Revised manuscript received May 20, 2008. Accepted June 12, 2008.

A multifaceted approach to atmospheric aerosol analysis is often desirable in field studies where an understanding of technical comparability among different measurement techniques is essential. Herein, we report quantitative intercomparisons of particle-induced X-ray emission (PIXE) and proton elastic scattering analysis (PESA), performed offline under a vacuum, with analysis by aerosol mass spectrometry (AMS) carried out in real-time during the MCMA-2003 Field Campaign in the Mexico City Metropolitan Area. Good agreement was observed for mass concentrations of PIXE-measured sulfur (assuming it was dominated by SO_4^{2-}) and AMS-measured sulfate during most of the campaign. PESA-measured hydrogen mass was separated into sulfate H and organic H mass fractions, assuming the only major contributions were $(NH_4)_2SO_4$ and organic compounds. Comparison of the organic H mass with AMS organic aerosol measurements indicates that about 75% of the mass of these species evaporated under a vacuum. However ∼25% of the organics does remain under a vacuum, which is only possible with low-vapor-pressure compounds, and which supports the presence of high-molecular-weight or highly oxidized organics consistent with atmospheric aging. Approximately 10% of the chloride detected by AMS was measured by PIXE, possibly in the form of metal−chloride complexes, while the majority of Cl was likely present as more volatile species including NH_4Cl. This is the first comparison of PIXE/PESA and AMS and, to our knowledge, also the first report of PESA hydrogen measurements for urban organic aerosols.

Introduction

Quantification and characterization of atmospheric aerosols presents many challenges. The complexity and variety of aerosol components, their transport, and chemical reactivity often require a multifaceted approach to analysis. Many important advances in analytical instrumentation for atmospheric research have been achieved over the past several decades, including both "offline" laboratory analyses of collected samples, and "online," or real-time, measurements. Intercomparison of different analysis methods is crucial for data comparability and may be enabled by field studies where typically a variety of different techniques are employed.

Particle-induced X-ray emission (PIXE) is a highly sensitive and efficient means of analyzing the elemental composition of bulk samples of atmospheric aerosols (*1*). This technique involves irradiation of the sample with energetic protons, causing the emission of X-rays characteristic of elements present in the sample. Complementary information may be collected by proton elastic scattering analysis (PESA), which provides hydrogen mass concentrations through measurements of forward proton scattering (*2, 3*). Both methods are commonly used for the analysis of aerosol samples collected by a DRUM (Davis Rotating-drum Uniform-size-cut Monitoring) impactor onto continuously moving substrates capable of following chemical changes in aerosol composition in a time-resolved manner (*4*). Several limitations of the PIXE/PESA analyses must be considered, namely, the loss of semivolatile compounds under a vacuum during analysis and the inability to determine the molecular form of individual elements.

The Aerodyne aerosol mass spectrometer (AMS) provides size and compositional information on submicron, nonrefractory aerosols at a time resolution of ∼2 min for the quadrupole version of the instrument (Q-AMS) (*5, 6*) and down to a few seconds with the Q-AMS single-ion monitoring mode (*7*) and newer time-of-flight versions (*8*). The AMS operates by drawing atmospheric aerosols into a series of vacuum chambers for chemical compositional analysis and size measurement based on particle time-of-flight. A collection of particles is flash-vaporized by impact onto a hot surface under a high vacuum; the vapor species are ionized by electron impact, and the ions are detected with a mass spectrometer. The main limitations of the AMS are its inability to detect refractory species (i.e., dust, sea-salt, soot) and supermicron particles and the need to apply an empirical correction for particle bounce at its vaporizer. Its main strengths are time and size resolution, quantitative analysis, and the ability to separate several types of inorganic and organic species (*9*).

The Mexico City Metropolitan Area (MCMA) field campaign took place in April, 2003 (MCMA-2003) as a collaborative effort among different research groups to analyze the chemical composition, dispersion, and atmospheric processing of atmospheric pollutants through a comprehensive network of gas-phase, aerosol, and meteorological measurements (*10*). The unique topographical, meteorological, and pollution characteristics of MCMA have been discussed previously (*10–12*). The collocation of a DRUM impactor used

* Corresponding author e-mail: kirstenj@alum.mit.edu.
† Massachusetts Institute of Technology.
‡ Pacific Northwest National Laboratory.
§ University of Colorado.
∥ Molina Center for Energy and the Environment.
⊥ Universidad Autonoma del Estado de Morelos.
Now at Finnegan, Henderson, Farabow, Garrett & Dunner, L.L.P., Washington, DC 20001.
▽ Now at Department of Chemistry and Biochemistry, University of California—San Diego, La Jolla, California 92093.

10.1021/es800393e CCC: $40.75
Published on Web 07/25/2008

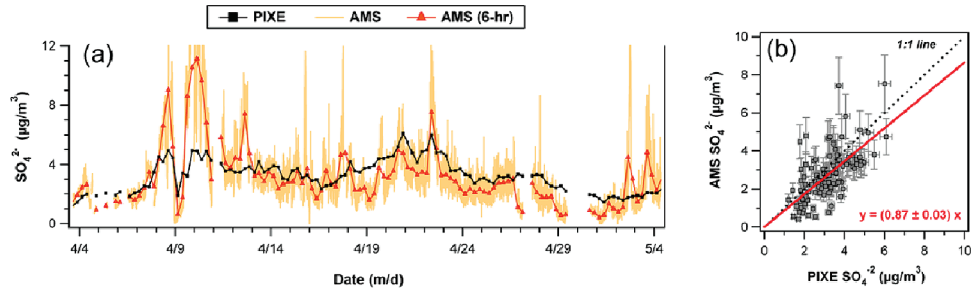

FIGURE 1. (a) Time series for SO_4^{2-} measured by PIXE and AMS during MCMA-2003. (b) PIXE vs AMS measurement of SO_4^{2-} excluding April 8−12th; $R^2 = 0.62$.

for PIXE/PESA sample collections and an AMS provided a unique opportunity for intercomparison of these techniques. PIXE/PESA and AMS employ fundamentally different methods of analysis yet provide remarkably complementary data. PIXE's sensitivity to high Z elements and inability to measure semivolatile compounds are inversely mirrored by the AMS detection of only nonrefractory aerosols that vaporize under a high vacuum at temperatures ≤ 600 °C. We have previously reported chemical characterization and source apportionment of $PM_{2.5}$ with these techniques independently (*13–15*). Herein, we report quantitative comparisons of these techniques to contribute to the understanding of urban aerosol characteristics, as well as to explore differences between these two measurement methods.

Experimental Section

PIXE/PESA. Samples of size-segregated $PM_{2.5}$ were collected at the ground-based MCMA- 2003 campaign supersite at the Centro Nacional de Investigación y Capacitación Ambiental (CENICA) in southeastern MCMA (*13*). Aerosol samples were collected continuously from April 3rd to May 4th onto Teflon strip substrates using a three-stage DRUM impactor, sampling into three separate size ranges: 1.15−2.5 μm (stage A), 0.34−1.15 μm (stage B), and 0.07−0.34 μm (stage C) (*4*). PIXE, PESA, and scanning transmission ion microscopy (STIM) analyses were carried out within several weeks following MCMA-2003 at the Environmental Molecular Sciences Laboratory located at the Pacific Northwest National Laboratory (PNNL). Aerosol collection and experimental procedures are described elsewhere (*3, 13*). Briefly, PIXE and PESA analyses were carried out simultaneously under a vacuum (2×10^{-7} Torr) with a 3.5 MeV proton beam. Samples were placed under a vacuum for about 30 min before, and 2.5 h during, analysis. PIXE spectra were evaluated by the GUPIX program (*16*), and mass concentrations of elements Na to Pb were determined by calibration to known standards with 5% uncertainty for major elements (S, Si, and K). Hydrogen concentrations were determined from PESA spectra with reference to Mylar ($C_{10}H_8O_4$) films of known thicknesses. The results are expressed as time series of elemental mass concentrations of particulate material at a 6 h time resolution.

AMS. A Q-AMS was deployed at CENICA during MCMA-2003. The instrument has been described in detail elsewhere (*5, 6, 17*). Air was sampled and analyzed continuously through a 9-m-long inlet as described by Salcedo et al. (*14*). The aerosol size measurement was calibrated using NIST-traceable polystyrene latex spheres (Duke Scientific), while the concentration measurement was calibrated by sampling dry size-selected ammonium nitrate particles as described by Jimenez et al. (*6*). Concentrations of species other than ammonium and nitrate were calculated using relative ionization efficiencies determined in previous laboratory calibrations (*18*). Data were analyzed in Igor Pro using the standard Q-AMS analysis software; the main scientific and technical results are discussed in detail elsewhere (*10, 14, 15, 19–23*).

The AMS has ~100% transmission efficiency for particles 60−600 nm in vacuum aerodynamic diameter (d_{va}) with partial transmission up to 1.5 μm; the total size range is thus approximately PM_1 (*14*). Particle shape and density are important parameters that affect aerodynamic sizing; the following expression relates d_{va} (relevant in the free molecular regime used in AMS detection) with the continuum regime aerodynamic diameter, d_{ca} (approximately applicable to the size cuts of the DRUM impactor):

$$d_{va} = d_{ca}\sqrt{\frac{\rho_p}{\chi\rho_o}}$$

where ρ_p is the particle density, $\rho_o = 1$ g cm^{-3} is the standard density, and χ is the dynamic shape factor, with $\chi = 1$ for a sphere and $\chi > 1$ for irregular particles such as soot aggregates (*24*). Given the most comparable size range of the PIXE/PESA data determined by the DRUM sampling, 0.07 μm ≤ d_{ca} ≤ 1.15 μm (sum of stages B and C), a systematic difference in measured mass is expected.

Results and Discussion

Sulfate. Due to its very low vapor pressure at ambient temperature, ammonium sulfate is measured quantitatively by PIXE as elemental S. The AMS can also measure this species quantitatively due to its rapid evaporation under the AMS operating conditions. Considering that $(NH_4)_2SO_4$ is the dominant sulfur-containing aerosol type in the MCMA (*14, 25*), a direct comparison of the two instrumental techniques was possible. The PIXE sulfate mass was estimated by assuming that all sulfur was present as sulfate (SO_4^{2-}) according to $[SO_4^{2-}]_{PIXE} = 3[S]_{PIXE}$.

The sulfate time series comparison (Figure 1a) shows agreement in the overall concentration profiles; however, the PIXE concentrations are somewhat higher most of the time, as expected from the difference in the aerosol collection size ranges. A discrepancy extending from April 8−12th is evident where AMS measurements are up to a factor of 2 higher; possible explanations are explored below. Excluding this period gives the $x-y$ correlation shown in Figure 1b, which captures the tendency toward PIXE values with $y = (0.87 \pm 0.03)x$ by least-squares linear regression, $R^2 = 0.62$ ($n = 101$). This suggests that the fraction of the sulfate mass missed by the AMS due to particles larger than its transmission range in this campaign was small, supported by comparison of the AMS and the optical counter size distributions reported by Salcedo et al. (*26*).

In contrast to the majority of the campaign where aerosols were effectively neutralized by an abundance of NH_3 (*22*), aerosols over April 8−12th were substantially acidic. An ion balance of AMS data shows that the measured NH_4^+ was lower than the amount required to fully neutralize sulfate ($(NH_4)_2SO_4$), nitrate (NH_4NO_3), and chloride (NH_4Cl) (*14*). Because sulfuric acid has a low vapor pressure, it readily partitions to the aerosol phase where the preferred form is solid or aqueous $(NH_4)_2SO_4$. In the case of insufficient gas-phase NH_3, the aerosol remains partially acidic, containing NH_4HSO_4 and possibly H_2SO_4. This "acidic period" coincides with pronounced industrial emissions, including the maxi-

mum SO_2 concentration of the MCMA-2003 campaign (*13*). The relative humidity (RH) during this period was also relatively high, with overnight RH levels reaching up to 90%, which would be expected to enhance the sulfate production rate. The boundary layer during the MCMA-2003 campaign was roughly 3000 m with thermal inversions around 100 m (*12*). An overnight thermal inversion may have delayed mixing between sulfate produced from SO_2 industrial emissions aloft and NH_3, whose sources (e.g., sewage) are ground-based.

The observed discrepancies during the acidic period warrant further discussion. From the perspective of PIXE detection, a heterogeneous reaction between the sample surface and SO_2 could have caused a mass artifact considering that no denuder was used to remove reactive gases from our sampling line prior to aerosol collection. This type of interaction would most likely have increased, rather than decreased, the amount of sulfur detected by PIXE, however. Additionally, Eldred and Cahill (*27*) found no evidence to support such an artifact. A more plausible explanation involves the reduced pressure and/or proton beam conditions employed during PIXE analysis. Richter et al. (*28*), following work by Hansen et al. (*29*), studied the thermal decomposition of H_2SO_4, NH_4HSO_4, and $(NH_4)_2SO_4$ as a function of proton beam current density, substrate, and pressure in the PIXE chamber. They recorded losses up to 50% caused by localized heating of the sample upon exposure to the proton beam, and minor losses due to pressure within the range 4×10^{-4} to 7.5×10^{-2} Torr. Because our analysis employed a smaller current (0.2 nA/cm^2 vs 150 nA/cm^2) and thinner substrates ($\sim$0.6 mg/cm^2 vs 5 mg/cm^2), minimal loss was anticipated in our analysis. Given the different conditions between our study and that of Richter et al., however, we cannot preclude a loss of partially acidic aerosol during PIXE analysis.

From the AMS perspective, dry particles dominated by components of lower volatility may bounce after impacting the vaporizer, lowering the bounce-related collection efficiency (E_b) (*17*). Given the observed composition during MCMA-2003 and the E_b-composition relationships derived from previous measurements, a total collection efficiency (CE) of 0.5 was assumed for the AMS. E_b can increase for very acidic ambient particles (mixtures of NH_4HSO_4 and H_2SO_4), but it stays constant at $\sim$0.5 for NH_4HSO_4 and less acidic particles (*30*). Since the particles measured during the acidic period in Mexico City were not more acidic than NH_4HSO_4 (*14, 22*), a value for E_b exceeding 0.5 was not expected. The AMS quantification was verified using intercomparisons with other instruments. Comparisons with DustTrak (Figure 2a in ref *14*) and LASAIR (Figure 9a in ref *26*) do not show a systematic difference between the acidic period and the neutralized periods like the one in Figure 1 above. Thus, it appears unlikely that variations in the AMS CE can provide an explanation.

There is currently no evidence for significant concentrations of organosulfate or metal sulfate compounds during MCMA-2003, but we cannot completely rule out these possibilities. The former may have evaporated under a vacuum prior to PIXE analysis, while the latter could have escaped AMS detection if they were not vaporized.

PESA Hydrogen and AMS Organics. Salcedo et al. (*14*) report that $\sim$55% of the total $PM_{2.5}$ mass during MCMA-2003 was attributed to organic compounds, with an additional 11% contribution from black carbon (BC). Although carbon was not directly detected by PIXE/PESA, it was inferred from STIM that about 50% of the nonvolatile $PM_{2.5}$ was carbonaceous, including both organic carbon and BC, after accounting for the contribution of inorganics estimated from the PIXE data (*13*). PESA-measured H is a useful marker for organic compounds otherwise undetected by PIXE. Since the vapor pressure of organic compounds determines their relative tendency to evaporate or remain in the particle phase

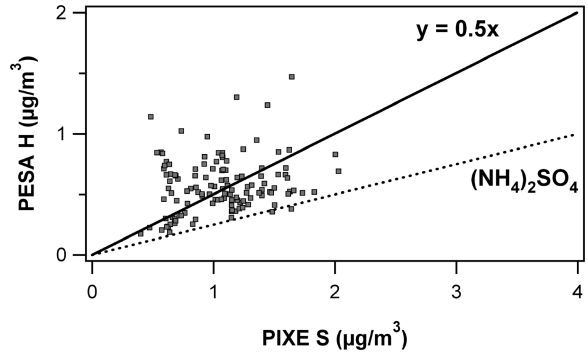

FIGURE 2. PIXE sulfur vs PESA hydrogen for stages B and C (0.07 μm $\leq$ d_a $\leq$ 1.15 μm).

under a vacuum, PESA also provides insight into the nature of organic compounds. Total H mass was apportioned to $(NH_4)_2SO_4$ and organic compounds, assuming a complete loss of water, NH_4NO_3, and NH_4Cl under a vacuum, and in the absence of any other major sources of hydrogen, neglecting a small amount of H in BC. Mass fractions of "sulfate H" and "organic H" were therefore calculated from PESA and PIXE data as follows:

$$sulfate\ H = \underbrace{\frac{8 \cdot aw_H}{aw_S}}_{=0.25} \cdot [S]_{PIXE}$$

$$organic\ H = [H]_{PESA} - sulfate\ H$$

$$\text{organic H} = [H]_{\text{PESA}} - \text{sulfate H}$$

where aw_H and aw_S are the atomic weights of hydrogen and sulfur, respectively. An excess of H over that accounted by $(NH_4)_2SO_4$ is apparent in Figure 2. Because BC is expected to make a minor contribution to the PESA-measured H mass, a distinction between organic and BC H has not been made. For example, given the 2.2 μg/m^3 average concentration of soot during MCMA-2003 (*14*) and estimating $\sim$1% hydrogen in BC by mass (*31*), soot would account for less than 5% of PESA-measured organic H. Note that organic H includes organic compounds adsorbed or condensed on the BC surface.

Figure 3a shows the time series for organic H and sulfate H from PESA measurements along with the time series of organic mass measured by AMS; axes are scaled for visual comparison purposes. A correction has been made in the hydrogen apportionment for NH_4HSO_4 during the aforementioned acidic period. PESA organic H exhibits a strong diurnal trend, whereas sulfate H shows a much flatter temporal profile indicative of the regional character of this species lacking major sources inside the city (*14, 25*). The organic H concentration peaks during late morning to early afternoon, likely related to both primary anthropogenic emissions and secondary organic aerosol (SOA) formation through photochemical reactions (*15, 25*).

Apparent correlation between scaled organic H and AMS organics' time series validates our assumptions on hydrogen source apportionment and indicates that a significant fraction of organic aerosol mass remained under a vacuum for PESA analysis. The two sets of measurements may be described by a linear fit, $y = (36.92 \pm 2.77)x + (6.06 \pm 0.49)$, $\chi^2 = 120$ (Figure 3b), assuming 20% uncertainty in each coordinate (*32*). The $\sim$6 μg/m^3 offset is consistent with loss of more-volatile organics under a vacuum.

Multivariate analysis of the AMS data has enabled a greater in-depth interpretation of complex organic spectra. Zhang et al. (*33*) deconvoluted the total AMS organic aerosol mass into two components: hydrocarbon-like organic aerosol

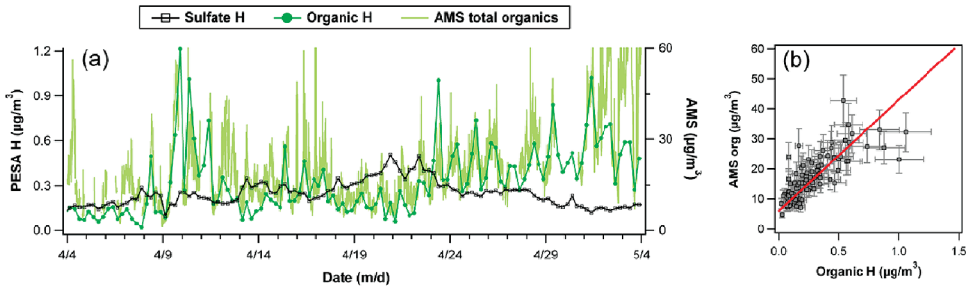

FIGURE 3. (a) Time series of PESA organic H and sulfate H, and AMS total organic mass. (b) PESA organic H vs AMS total organics with $y = (36.92 \pm 2.77)x + (6.06 \pm 0.49)$, $\chi^2 = 120$; $R^2 = 0.59$ ($n = 96$).

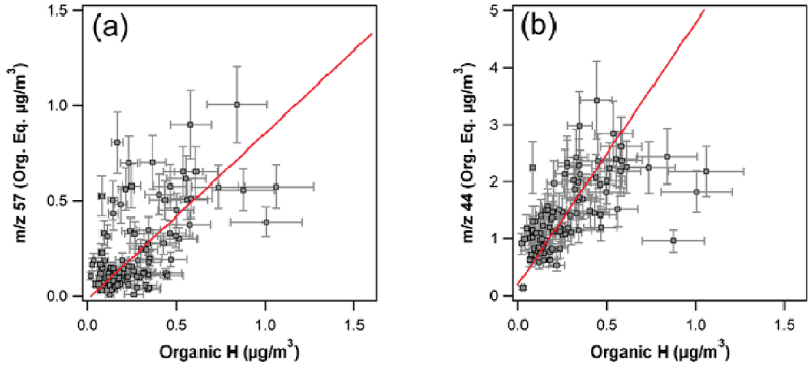

FIGURE 4. Correlation between PESA organic H and AMS organic measurements: (a) m/z 57, a tracer of HOA and primary BBOA, $y = (0.87 \pm 0.06)x - (0.02 \pm 0.01)$, $\chi^2 = 529$; $R^2 = 0.33$ ($n = 96$). (b) m/z 44, a tracer of OOA/SOA, $y = (4.59 \pm 0.26)x + (0.19 \pm 0.03)$, $\chi^2 = 250$; $R^2 = 0.37$ ($n = 96$).

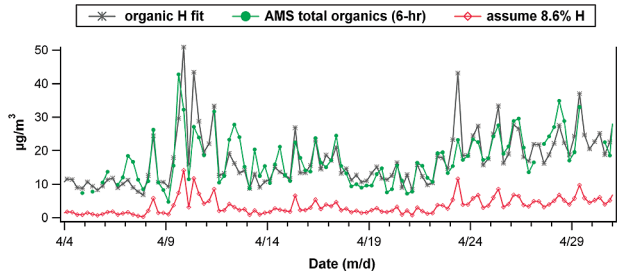

FIGURE 5. Total organic aerosol mass obtained via PESA-measured organic H.

(HOA), traced by m/z 57 (mainly $C_4H_9^+$), related to primary urban and biomass burning emissions, and oxygenated organic aerosol (OOA), traced by m/z 44 (mainly CO_2^+), exhibiting a much greater oxygen content mainly due to SOA formation (*24, 34*). The individual correlations for each tracer m/z with PESA organic H are shown in Figure 4. Although HOA is expected to contribute relatively more hydrogen because of its greater degree of saturation (*34*), recent results from Mexico City indicate that HOA and biomass-burning OA (BBOA) are more volatile than OOA (*35*). Thus, HOA and BBOA are likely preferentially lost by evaporation under a vacuum during PESA, which presumably drives the higher correlation of organic H with the OOA/SOA tracer.

The average concentration of nonvolatile organics may be inferred from PESA data based on the estimates of an average H content in total organic mass during the campaign. Applying results from Zhang et al. (*33*) indicating an average HOA composition of C/H = 1:1.9 and OOA composition of C/H/O = 1:1.6:0.8 for urban aerosol in Pittsburgh, and given that HOA and OOA comprised about 1/3 and 2/3, respectively, of the total organic aerosol mass during MCMA-2003 (*14*), an average of 8.6% H may be estimated. Figure 5 compares this organic H scaling method with the AMS-measured organics time series. The quantitative offset evident in the graph emphasizes the fact that MCMA organic aerosols encompass a range of vapor pressures, and their evaporation under a vacuum during PESA analysis is significant. Figure 5 also shows a total organic mass retrieved from PESA organic H via the linear fit with AMS organics (Figure 3b), which provides much better agreement.

Although PIXE has been used extensively in atmospheric aerosol measurement, few studies have adopted PESA hydrogen as a marker for organic compounds. The IMPROVE (Interagency Monitoring of Protected Visual Environments) network is a notable exception in which PESA hydrogen measurements are applied to quantify the total organic mass in a comprehensive chemical speciation of $PM_{2.5}$ and PM_{10} in U.S. national parks (*36*). PESA data obtained under a vacuum for aerosol samples collected on nylon filters are

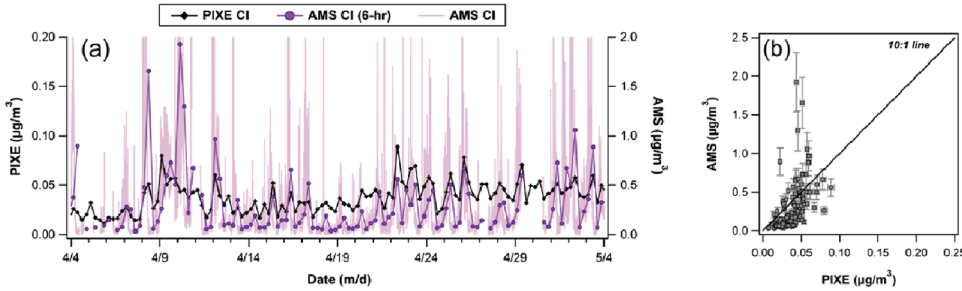

FIGURE 6. (a) PIXE and AMS Cl time series (note the different y-axis scales). (b) PIXE vs AMS Cl; $R^2 = 0.25$ ($n = 114$).

compared to organic carbon mass concentrations measured independently by thermal optical reflectance at atmospheric pressure for samples collected on quartz filters. The IMPROVE data analysis procedure involves multiplying the PESA hydrogen concentrations by a factor of 11 to determine the total organic mass, which corresponds to an average 9% H content (empirical formula $C_9H_5O_2$), similar to our assumption in Figure 5. This method has shown favorable agreement even though allowances were not made for sample loss at the reduced pressures employed during PESA (*37*). Organic aerosol concentrations recorded in these remote U.S. parks range from 1 to 5 $\mu g/m^3$, or roughly 1/10 the concentrations measured during MCMA-2003 ($\sim$20 $\mu g/m^3$). Organic aerosols in rural and remote locations such as national parks tend to be extensively oxidized (*38, 39*), the type of organic aerosol which shows the lowest volatility (*35*) likely due to extensive atmospheric processing after long residence times. In contrast, Mexico City has significant concentrations of primary combustion, biomass burning, and fresh SOA, which are more volatile than aged OOA (*35*). This likely explains why a simple scaling of PESA-measured hydrogen is not valid in our case. Figure 5 clearly illustrates a difference on the order of 10 $\mu g/m^3$. From the slope of the linear fit in Figure 3b, and assuming an average 8.6% H, we estimate that nonvolatile organics comprised $\sim$25% of the total organic mass during MCMA-2003.

Chlorine/Chloride. A quantitative comparison of elemental Cl from PIXE and AMS provides information on the sources and chemical form of chlorine-containing aerosols sampled during MCMA-2003. The respective time series appear in Figure 6a (note the different axis ranges) showing coincident diurnal trends with the maximum concentrations reached overnight to early morning hours. The substantial mass difference indicates a semivolatile character to the aerosols, however, where PIXE Cl accounts for about 10% of the AMS Cl mass (Figure 6b). Particulate chlorine may come from a variety of sources for in-land urban locations such as the MCMA. Salcedo et al. (*14*) attributed aerosol Cl to water treatment and refuse burning, primarily as NH_4Cl formed from neutralization reactions between HCl and NH_3. NH_4Cl appears to have a semivolatile character in ambient air (*14*) and readily evaporates at reduced pressure, consistent with the observations shown in Figure 6. The degassing of HCl (*40*) followed by drying of the PIXE sample under a vacuum may also explain some Cl loss; however, AMS data offer support for NH_4Cl. Evidence of regional fires and correlations observed among markers for biomass burning emissions (K, Cl, Br) suggest an additional source of Cl particulate mass during the campaign (*13, 14*). PIXE-measured Cl concentrations were low ($\sim$40 ng/m^3) (*13*) and may be associated with low-volatility species such as metal chlorides or possibly potassium chloride in biomass burning emissions.

Acknowledgments

We are grateful to Rafael Ramos (RAMA) and CENICA personnel (especially Felipe Angeles and Salvador Blanco) for their help during the campaign. The MIT-MCE2-UCSD group acknowledges support from the Mexican Metropolitan Environmental Commission, National Science Foundation (ATM-0528227), and Department of Energy (Award DE-FG02-05ER63980). The CU group acknowledges support from NSF (ATM-0449815 and ATM-0528634) and the Atmospheric Science Program (Office of Biological and Environmental Research) of the U.S. Department of Energy (DE-FG02-05ER63981) and the U.S. EPA STAR (RD-83216101-0). The PNNL group acknowledges support from ASP/OBER DOE. PIXE and PESA analyses were performed in the Environmental Molecular Sciences Laboratory, a national scientific user facility sponsored by OBER/DOE and located at Pacific Northwest National Laboratory. PNNL is operated by the U.S. Department of Energy by Battelle Memorial Institute under contract DE-AC06-76RL0. This paper has not been reviewed by either agency, and thus no official endorsement should be inferred.

Literature Cited

(1) Johansson, S.; Campbell, J. L.; Malmqvist, K. G. *Particle-Induced X-Ray Emission Spectrometry (PIXE)*; John Wiley & Sons: New York, 1995.
(2) Bench, G.; Grant, P. G.; Ueda, D.; Cliff, S. S.; Perry, K. D.; Cahill, T. A. The use of STIM and PESA to measure profiles of aerosol mass and hydrogen content, respectively across Mylar rotating drums impactor samples. *Aerosol Sci. Technol.* **2002**, *36*, 642–651.
(3) Shutthanandan, V.; et al. Development of PIXE, PESA and Transmission Ion Microscopy capability to measure aerosols by size and time. *Nucl. Instrum. Methods B* **2002**, *189*, 284–288.
(4) Cahill, T. A.; Wakabayashi, P. Compositional analysis of size-segregated aerosol samples. *ACS Adv. Chem. Ser.* **1993**, *232*, 211–228.
(5) Jayne, J. T.; Leard, D. C.; Zhang, X.; Davidovits, P.; Smith, K. A.; Kolb, C. E.; Worsnop, D. R. Development of an Aerosol Mass Spectrometer for size and composition analysis of submicron particles. *Aerosol Sci. Technol.* **2000**, *33*, 49–70.
(6) Jimenez, J. L. et al. Ambient aerosol sampling using the Aerodyne Aerosol Mass Spectrometer. *J. Geophys. Res.* **2003**, *108* (D7), 8425; DOI: 10.1029/2001JD001213.
(7) Crosier, J.; et al. Technical Note: Description and use of the new Jump Mass Spectrum mode of operation for the Aerodyne Quadrupole Aerosol Mass Spectrometers (Q-AMS). *Aerosol Sci. Technol.* **2007**, *41*, 865–872.
(8) DeCarlo, P. F.; et al. Field-deployable, High-Resolution, Time-of-Flight Aerosol Mass Spectrometer. *Anal. Chem.* **2006**, *78*, 8281–8289.
(9) Zhang, Q.; Worsnop, D. R.; Canagaratna, M. R.; Jimenez, J. L. Hydrocarbon-like and oxygenated organic aerosols in Pittsburgh: Insights into sources and processes of organic aerosols. *Atmos. Chem. Phys.* **2005**, *5*, 3289–3311.
(10) Molina, L. T.; Kolb, C. E.; De Foy, B.; Lamb, B. K.; Brune, W. H.; Jimenez, J. L.; Molina, M. J. Air quality in North America's most populous city - overview of MCMA-2003 campaign. *Atmos. Chem. Phys.* **2007**, *7*, 2447–2473.
(11) Molina, L. T.; Molina, M. J. *Air Quality in the Mexico Megacity: An Integrated Assessment*; Kluwer Academic: Cambridge, 2002.
(12) de Foy, B.; Caetano, E.; Magana, V.; Zitacuaro, A.; Cardenas, B.; Retama, A.; Ramos, R.; Molina, L. T.; Molina, M. J. Mexico City basin wind circulation during the MCMA-2003 Field Campaign. *Atmos. Chem. Phys.* **2005**, *5*, 2267–2288.
(13) Johnson, K. S.; de Foy, B.; Zuberi, B.; Molina, L. T.; Molina, M. J.; Xie, Y.; Laskin, A.; Shutthanandan, V. Aerosol composition and source apportionment in the Mexico City Metropolitan Area with PIXE/PESA/STIM and multivariate analysis. *Atmos. Chem. Phys.* **2006**, *6*, 4591–4600.
(14) Salcedo, D.; et al. Characterization of ambient aerosols in Mexico City during the MCMA-2003 campaign with Aerosol Mass Spectrometry: Results from the CENICA Supersite. *Atmos. Chem. Phys.* **2006**, *6*, 925–946.
(15) Volkamer, R.; Jimenez, J. L.; San Martini, F.; Dzepina, K.; Zhang, Q.; Salcedo, D.; Molina, L. T.; Worsnop, D. R.; Molina, M. J. Secondary organic aerosol formation from anthropogenic air pollution: Rapid and higher than expected. *Geophys. Res. Lett.* **2006**, *33*, L17811.
(16) Maxwell, J. A.; Campbell, J. L.; Teesdale, W. J. The GUELPH PIXE software package. *Nucl. Instrum. Methods B* **1989**, *43*, 218–230.
(17) Canagaratna, M. R.; et al. Chemical and microphysical characterization of ambient aerosols with the Aerodyne Aerosol Mass Spectrometer. *Mass Spec. Rev.* **2007**, *26*, 185–222.
(18) Alfarra, M. R.; et al. Characterization of urban and regional organic aerosols in the Lower Fraser Valley using two Aerodyne Aerosol Mass Spectrometers. *Atmos. Environ.* **2004**, *38*, 5745–5758.
(19) Salcedo, D.; et al. Technical note: Use of a beam width probe in an Aerosol Mass Spectrometer to monitor particle collection efficiency in the field. *Atmos. Chem. Phys.* **2007**, *7*, 549–556.
(20) Marr, L. C.; et al. Sources and transformations of particle-bound polycyclic aromatic hydrocarbons in Mexico City. *Atmos. Chem. Phys.* **2006**, *6*, 1733–1745.
(21) Dzepina, K.; et al. Detection of particle-phase polycyclic aromatic hydrocarbons in Mexico City using an Aerosol Mass Spectrometer. *Int. J. Mass Spectrom.* **2007**, *263*, 152–170.

(22) San Martini, F. M.; et al. Implementation of a Markov Chain Monte Carlo Method to inorganic aerosol modeling of observations from the MCMA-2003 Campaign. Part II: Model application to the CENICA, Pedregal and Santa Ana sites. *Atmos. Chem. Phys.* **2006**, *6*, 4889–4904.
(23) Volkamer, R.; San Martini, F.; Molina, L. T.; Salcedo, D.; Jimenez, J. L.; Molina, M. J. A missing sink for gas-phase glyoxal in Mexico City: Formation of secondary organic aerosol. *Geophys. Res. Lett.* **2007**, *34*, L19807.
(24) DeCarlo, P. F.; Slowik, J. G.; Worsnop, D. R.; Davidovits, P.; Jimenez, J. L. Particle morphology and density characterization by combined mobility and aerodynamic diameter measurements. Part 1: Theory. *Aerosol Sci. Technol.* **2004**, *38*, 1185–1205.
(25) DeCarlo, P. F.; et al. Fast airborne aerosol size and chemistry measurements with the High Resolution Aerosol Mass Spectrometer during the MILAGRO Campaign. *Atmos. Chem. Phys. Discuss.* **2007**, *7*, 18269–18317.
(26) Salcedo, D.; et al. Characterization of ambient aerosols in Mexico City during the MCMA-2003 campaign with aerosol mass spectrometry. Part I: quantification, shape-related collection efficiency, and comparison with collocated instruments. *Atmos. Chem. Phys. Discuss.* **2005**, *5*, 4143–4182.
(27) Eldred, R. A.; Cahill, T. A. Sulfate sampling artifact from SO_2 and alkaline soil. *Environ. Sci. Technol.* **1997**, *31*, 1320–1324.
(28) Richter, F. W.; Ries, H.; Watjen, W. On the problem of sulfur losses during PIXE analysis. *Nucl. Instrum. Methods B* **1984**, *3*, 151–153.
(29) Hansen, L. D.; Ryder, J. F.; Mangelson, N. F.; Hill, M. W.; Faucette, K. J.; Eatough, D. J. Inaccuracies encountered in sulfur determination by Particle Induced X-ray Emissions. *Anal. Chem.* **1980**, *52*, 821–824.
(30) Quinn, P. K.; et al. Impacts of sources and aging on submicrometer aerosol properties in the marine boundary layer across the Gulf of Maine. *J. Geophys. Res.* **2006**, *111*, D23S36.
(31) Pantea, D.; Brochu, S.; Thiboutot, S.; Ampleman, G.; Scholz, G. A morphological investigation of soot produced by the detonation of munitions. *Chemosphere* **2006**, *65*, 821–831.
(32) Press, W. H. *Numerical Recipes in C: The Art of Scientific Computing*; Cambridge University Press: Cambridgeshire, U.K., 1992.
(33) Zhang, Q.; Alfarra, M. R.; Worsnop, D. R.; Allan, J. D.; Coe, H.; Canagaratna, M. R.; Jimenez, J. L. Deconvolution and quantification of hydrocarbon-like and oxygenated organic aerosol based on Aerosol Mass Spectrometry. *Environ. Sci. Technol.* **2005**, *39*, 4938–4952.
(34) Aiken, A. C. et al. O/C and OM/OC ratios of primary, secondary, and ambient organic aerosols with High Resolution Time-of-Flight Aerosol Mass Spectrometry. *Environ. Sci. Technol.* **2008**, *42*, 4478–4485.
(35) Huffman, J. A. et al. Volatility of primary and secondary organic aerosols in the field contradicts current model representations. *Environ. Sci. Technol.* Submitted.
(36) IMPROVE Data Guide http://vista.cira.colostate.edu/improve/ (accessed Jun 2008).
(37) Malm, W. C.; Sisler, J. F.; Huffman, D.; Eldred, R. A.; Cahill, T. A. Spatial and seasonal trends in particle concentration and optical extinction in the United States. *J. Geophys. Res.* **1994**, *99*, 1347–1370.
(38) Zhang, Q.; et al. Ubiquity and dominance of oxygenated species in organic aerosols in anthropogenically-influenced Northern Hemisphere Mid-latitudes. *Geophys. Res. Lett.* **2007**, *34*, L13801.
(39) Hand, J. L.; et al. Optical, physical and chemical properties of tar balls observed during the Yosemite Aerosol Characterization Study. *J. Geophys. Res.* **2005**, *110*, D21210.
(40) Yao, X.; Fang, M.; Chan, C. K. Experimental study of the sampling artifact of chloride depletion from collected sea salt aerosols. *Environ. Sci. Technol.* **2001**, *35*, 600–605.

ES800393E